

Report to CCTF from the National Measurement Institute, Australia

September 2006

1. UTC(AUS)

The history of UTC(AUS) over the last 2000 days is shown in Figure 1. NMIA's present policy is to maintain UTC(AUS) within 1 microsecond of UTC.

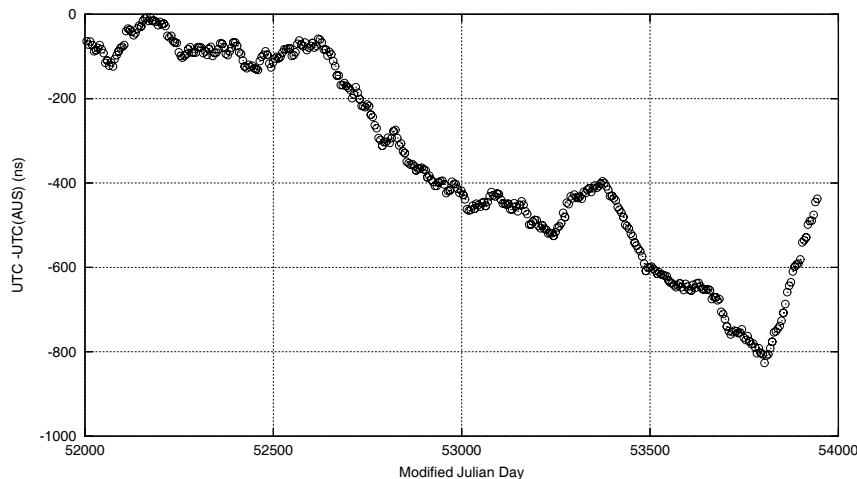


Figure 1. History of UTC(AUS) from April 2001 to August 2006. The rate of the Cs standard was adjusted on MJD 53804 (10/3/2006) to steer UTC(AUS) back towards UTC.

2. Two-way Satellite Time and Frequency Transfer (TWSTFT)

NMIA has actively participated in two-way satellite time and frequency transfer (TWSTFT) research in the Asia-Pacific region for many years. A long-running Ku-band link via PanAmSat PAS-8 to the National Institute of Information and Communications Technology (NICT) in Japan was upgraded in early 2003 to use the new multi-channel time-transfer modem developed by NICT. This link will be discussed in NICT's report. PanAmSat recently merged with Intelsat, so that PAS-8 is now an Intelsat satellite.

NMIA has also begun a series of trial observations with both NICT and the Telecommunications Laboratories (TL) in Taiwan, also made via PAS-8 using satellite time generously made available by NICT. The aim of this program is to compare observations with both the multi-channel NICT modem and a SATRE time-transfer modem, available at all three institutions.

3. GPS time-transfer

NMIA and its predecessor NML have supplied a number of time-transfer systems to calibration laboratories within Australia and to national measurement institutes around the Asia-Pacific region (Figure 2). At the time of writing there are over 30 such systems currently in operation in thirteen countries, with an accumulated total of over a hundred system-years of almost entirely trouble-free operation. This represents a significant body of experience and an important data resource. NMIA and other Asia-Pacific laboratories maintain extensive data archives which can be used to quantify the performance of time-transfer links generally and of several receivers specifically. It is worth noting here that there are two features of time-transfer links in this region which do not apply in (for example) Europe or North America, namely trans-equatorial links over long baselines and laboratories at mid-latitudes where ionospheric activity is particularly high.

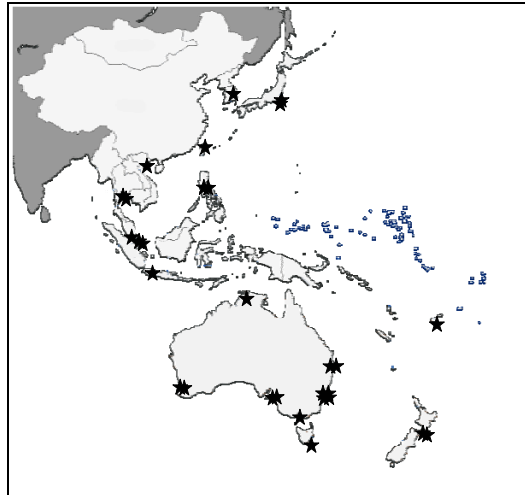


Figure 2. NMIA-developed GPS common-view time transfer systems installed in the Asia-Pacific region. In many cases these provide the primary link between the reference timescale of the host nation and UTC.

NMIA has also participated in a recent calibration campaign piloted by BIPM circulating an Ashtech Z12T geodetic receiver. For Javad geodetic receivers at NMIA, delays at L1 and L2 frequencies obtained by transfer from the calibrated Z12T show good agreement with an independent calibration carried out by NMIA using a GPS simulator made available by Australian Department of Defence. This is a particularly encouraging result in the context of the geodetic monitoring stations discussed in the following section.

4. Geodetic monitoring stations

A geodetic monitoring station has been constructed and commissioned at NMIA Lindfield, in a joint project with Australia's national mapping agency Geoscience Australia (GA). The station is based on a variant of the NMIA-developed time-transfer system, with the raw data from a Javad receiver processed both for geodesy (RINEX-format observation data) and time-transfer (CGGTTS-format timing data). The station contributes data to the Australian Regional GPS Network (ARGN) for mapping and geodesy, and also forms the SYDN node of the International GNSS Service (IGS) network. A recent position series obtained for the SYDN station is shown in Figure 3.

The station antenna is mounted in the grounds of the NMIA site at Lindfield, Sydney, on a concrete pillar extending approximately 10 m below ground level. A geodetic quality dual-frequency GPS receiver, the Javad/Topcon Euro-160, is sited in the time and frequency laboratory some distance away; this provides good access to reference clock signals and also stabilises the receiver temperature. The GPS signal is relayed from the antenna to the receiver over 520 m of optical fibre (Figure 4), to avoid signal attenuation and to minimise variation of delays with temperature.

We have conducted a series of tests to determine the variation of signal delays with temperature [R. B. Warrington *et al*, 2005 *Joint International Frequency Control Symposium and PTTI Systems and Applications Meeting*, tycho.usno.navy.mil/ptti/ptti2005/paper21.pdf]. These are important because the signal path includes additional components over a standard geodetic station, in particular the optical transceivers and fibre. The temperature tests compared CGGTTS-format GPS data files recorded for two dual-frequency Euro-160 receivers with a common antenna (zero baseline), with the component under test in one signal path placed in an environmental chamber and varied over a range from 0 to 40 °C.

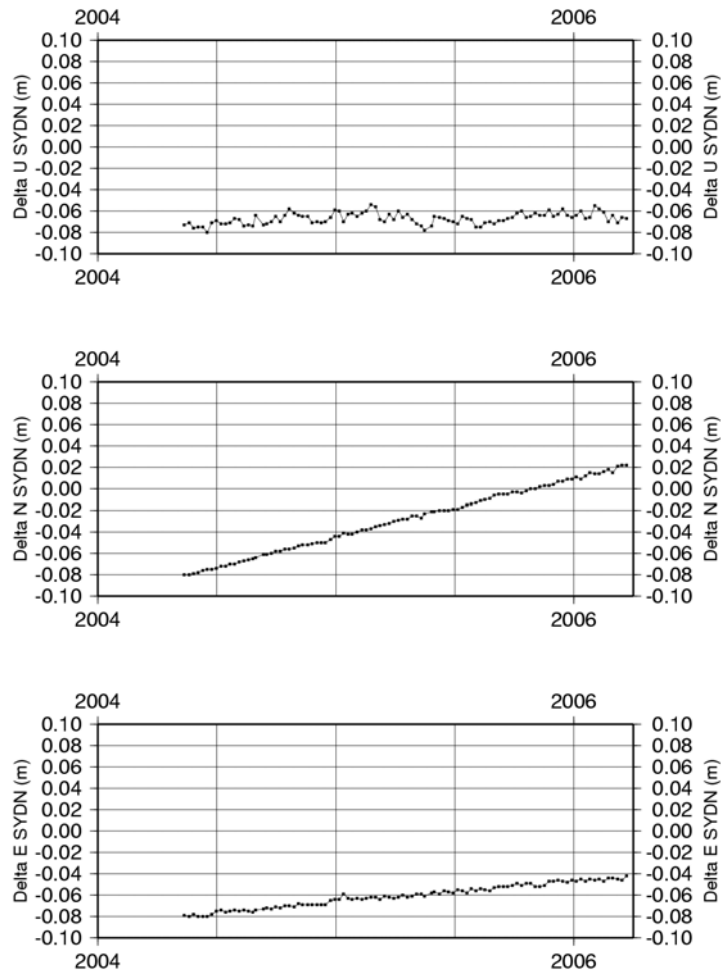


Figure 3. Position series for the SYDN node of the IGS network, on site at NMIA Lindfield, Sydney, from analysis by Geoscience Australia. The Australian plate is drifting predominantly northward at approximately 5 cm per year.

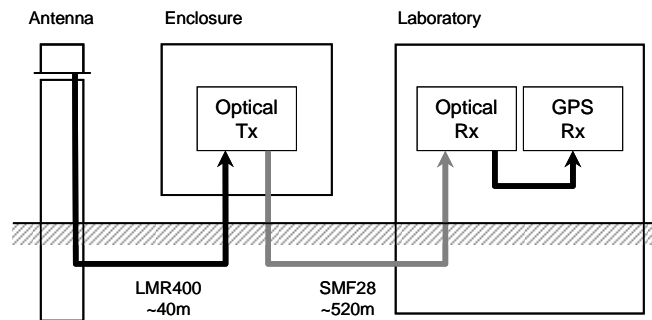


Figure 4. Design of the SYDN IGS station (not to scale). The GPS signal is carried from the choke-ring antenna over copper cable to an optical transmitter in a weatherproof enclosure, then by optical fibre to an optical receiver, and finally by a short copper cable to the GPS receiver. The horizontal line represents ground level.

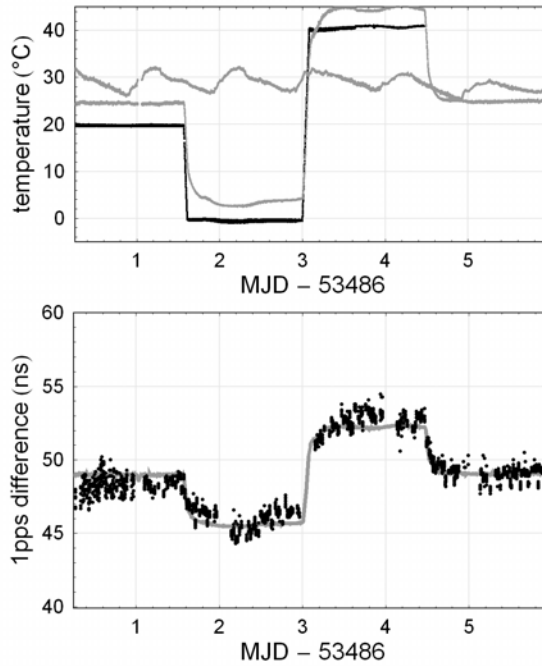


Figure 5. Testing the temperature dependence of GPS receiver internal delays (see text). The upper plot shows temperature of an environmental chamber (black) and of two receivers inside and outside the chamber (gray). The lower plot shows time differences between data tracks (points) from the two receivers; the fit (line) gives a coefficient of 160 ps/°C.

The results indicate no measurable temperature dependence for the optical transmitter (conservative upper limit 25 ps/°C). This is an important result, because this transmitter is in an outdoor environment and therefore subject to significant temperature variation. The variation of internal delay for the GPS receiver (Figure 5) was approximately 160 ps/°C, and therefore not significant as the receiver is in a temperature-controlled laboratory (typically ± 0.25 °C ambient). Finally the variation of optical fibre delay is similarly negligible (approximately 0.1 ps/°C per metre), especially since it is buried underground for much of its length and therefore subject to reduced temperature fluctuations.

A new station co-located with the radio telescope in Parkes, New South Wales has recently been commissioned in a collaboration between the Australia Telescope National Facility, GA and NMIA. The Parkes station uses the same receiver as the SYDN station and the same software developed by NMIA. The Parkes radio telescope undertakes extensive observations of millisecond pulsars.

5. Speaking clock systems

Two years ago, NMIA completed development of a “speaking clock” system capable of providing voice time announcements underpinned by hardware and software specifically designed to provide metrological integrity, at the point at which signals enter the public telephone network. This system was developed in response to a perceived need for a legally traceable telephone-based voice announcement time service.

The architecture is shown in Figure 6. Where the system is operated remotely from NMIA, a local atomic clock, linked back to NMIA by GPSCV, provides all critical timing signals for the system. In particular, marker pips in the time announcement are generated in hardware from these timing signals, to eliminate any software-induced delays or jitter. Time of day announcements are generated by the host PC and combined with the marker tones. The host PC also controls and monitors the external timing hardware. Leap seconds are handled automatically and Daylight Saving transitions are easily configurable.

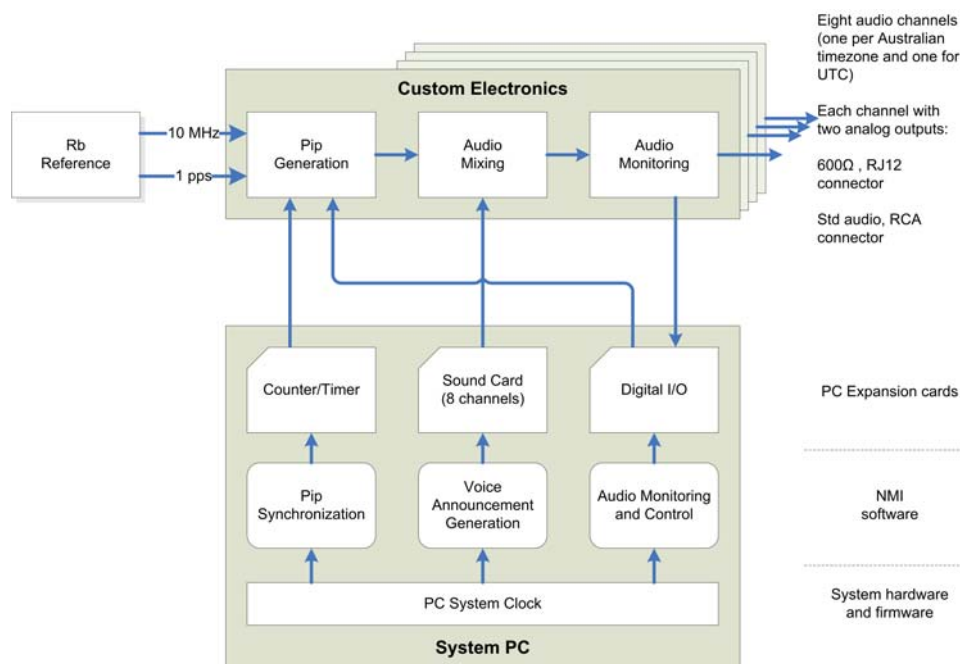


Figure 6. Architecture of the NMIA speaking clock system.

The present version of the system has eight audio outputs which are configurable for different offsets from UTC. More outputs can be provided if required. In Australia, seven outputs are required because there are three time zones, compounded by variations in implementation of Daylight Savings Time. In other countries where there is only one time zone, the extra channels could be used for announcements in different languages, for example.

The NMIA system now provides the Australian national Speaking Clock service, becoming operational in April 2006.

6. Traceable Network Time Protocol (NTP) systems

For many years NMIA has operated a national network of NTP servers, disseminating time to Australian users. The remote servers derive their time from the 1 pps output of a local atomic clock, linked back to UTC(AUS) via a GPSCV link. The internal clocks on the servers are traceable to UTC(AUS) with an uncertainty of $10\mu\text{s}$ as demonstrated by measurement of signals generated by software.

In Australia, there has been increasing interest by organizations in establishing traceability of Network Time, as realized within their network and on their computer systems, to UTC(AUS). This has been driven by an increasing awareness of the importance of high integrity timestamps on a wide variety of ICT-based business transactions. NMIA has recently supplied traceable NTP servers to a national telecommunications provider to establish traceability for their billing services. We have also commenced construction of traceable NTP servers for an Australian Government project to supply electronic notarisation services to Government and business.

7. Asia-Pacific Metrology Program (APMP) Activities

A portable version of the time transfer system was developed at NMIA in 2002, under contract to the Telecommunications Laboratories (TL) in Taiwan. The system was developed to support an international intercomparison of the internal delays of GPSCV time-transfer receivers. The portable system includes several additional features designed for this application, in particular a very rugged shock-mount case to protect the system during

shipping and stabilisation of the receiver temperature for best performance. A dual-frequency receiver allows accurate self-survey of the antenna coordinates of the portable system by post-processing of RINEX data to centimetre level, so that these need not be known in advance.

In 2004, 2005 and 2006 NMIA has been coordinating an extended series of comparisons within the Asia Pacific Metrology Programme (APMP), the network of national measurement institutes in the Asia-Pacific region. At the time of writing the system has visited seventeen laboratories (some more than once) in ten countries, representing essentially all the APMP members active in the field of time and frequency. A report on the first tour of the NMIA system is attached as an appendix. The delay of the portable system has been determined by comparison to receivers of the BIPM at the Observatoire de Paris, and of NIST in Colorado. We observe good agreement between these independent calibrations, and good stability of the receiver delay across an extended series of comparisons at NMIA. This calibrated delay can then be transferred to the primary receiver at each APMP national institute. The intercomparison provides important support for developing economies in the Asia-Pacific, and also establishes a formal comparison between the APMP and the equivalent regional organisations in Europe (EUROMET) and North America (SIM).

8. $^{171}\text{Yb}^+$ Trapped Ion Frequency Standard

Work on the NML 12.6 GHz $^{171}\text{Yb}^+$ trapped-ion frequency standard has continued slowly, as permitted by the other responsibilities of the Time and Frequency group. A new non-magnetic UHV chamber constructed of the novel alloy CrCu has been commissioned, and as expected has significantly reduced systematic uncertainties associated with magnetic field gradients. These were the dominant components in the most recent measurement of the 12.6 GHz transition frequency, and now contribute less than 1×10^{-15} to a projected combined uncertainty of 4×10^{-15} or below. We are also exploring the use of semiconductor laser diode systems to generate light near the 369 nm Yb^+ resonance transition, with the relatively recent advent of high-power near-UV laser diodes.

9. Collaboration with the University of Western Australia

The Frequency Standards and Metrology Group at the University of Western Australia (UWA) is well-known for its development of ultra-stable cryogenic oscillators. Clock ensembles at UWA and NMIA are to be compared for the first time by new TWSTFT and GPS carrier-phase time transfer links, currently being commissioned. The comparison between the two methods should provide important verification of performance, and allow optimisation of link parameters and data processing.

The UWA-NMIA links are being established in preparation for participation in the Atomic Clock Ensemble in Space (ACES) mission. UWA and NMIA form the only ACES User Group in the southern hemisphere.

10. New frequency comb

NMIA has recently purchased and commissioned a frequency comb based on erbium fibre-laser technology from Menlo Systems. The comb can be used to make absolute optical frequency measurements in the range 500 to 2000 nm. Initially it will be used to support the Length metrology programme by providing a reference for lasers used in gauge block calibration.

11. Training

NMIA has run two-day training courses in aspects of time and frequency measurement in November 2003 and April 2006, attended by staff from Australian calibration laboratories. A monograph incorporating the course material is under development. NMIA has also proposed an APMP seminar on time and frequency measurement; discussions regarding the timing and venue for this seminar are currently in progress.

12. Structure of the Time and Frequency Group

The Physical Metrology Branch of NMI is led by Dr Peter Fisk. The Time and Frequency group is led by Dr Bruce Warrington, with Senior Research Scientist Dr Michael Wouters and project officers Mr Michael Lawn, Mr Anura Gajaweera, Mr Stephen Quigg and Mr John Thorn.

APMP Round-Robin Intercomparison of GPS Receiver Delays

Report on the First Round, January to July 2004

R. B. Warrington, P. T. H. Fisk and M. J. Wouters



Australian Government

**National Measurement
Institute**

PO Box 264
Lindfield, NSW 2070
Sydney, Australia

1. Introduction

Between January and July of 2004, NMI Australia coordinated an intercomparison of GPSCV time-transfer receivers at several APMP member institutes. The purpose was to compare the internal receiver delays by circulating a common travelling receiver among the participating laboratories. The portable receiver was developed by staff at NMI under contract to the Telecommunications Laboratories in Taiwan, who generously made the receiver available for the campaign.

This report summarizes the results of the intercomparison, based on processing carried out at NMI. These results should be regarded as preliminary until all of the participating laboratories have had an opportunity to comment on the results. All data and analysis files are available on the NMI FTP site.

2. Schedule

The schedule of the first round of the comparison is shown in Table 1, which also includes details of the host receiver at each laboratory. Additional information about the set-up of equipment at each location is provided in Appendix 1.

Following commissioning at NMI, the portable system was operated at BNM-SYRTE in Paris. The host receiver of the Observatoire de Paris (OP) there has acted as reference for previous intercomparisons coordinated by the BIPM. We adopt the internal delay of this receiver as the reference for this intercomparison.

The portable system was returned to NMI after operation at BNM-SYRTE and also at the end of the first round, to verify consistency of the measurements.

3. Comparison procedure

The portable time-transfer system is a variant of the systems developed at NMI based on the Javad/Topcon Euro-80 dual-frequency GPS receiver [1]. This system processes raw receiver and timing data to generate output files in the standard CCTF format [2], but can also generate geodetic observation files in the standard RINEX format [3] from the same data. These files can be used for accurate self-survey of antenna coordinates. All raw data is stored by the system, allowing post-processing with antenna coordinates of the highest precision; these only become available when the International GPS Service finalises high-precision orbitography for the GPS satellites, some time after the data is recorded.

The equipment circulated comprised the receiver, its antenna and an antenna cable of known delay. A line amplifier was also circulated, to compensate for additional attenuation where a longer antenna cable was needed. Each host laboratory supplied two signals to the portable system: a 10 MHz reference frequency, and a 1 pulse-per-second signal derived from the local reference, $UTC(k)$, via a cable of known delay. In each laboratory the portable receiver was connected to the same clock as the host receiver.

CCTF data from both the host and portable receivers was returned to NMI for processing. The portable system includes a Zip drive, so that the larger raw data files could also be returned to NMI for post-processing. TL and NICT provided data for two host receivers during the comparison; in both cases, the analysis has only been carried out to date for one of the two.

Each laboratory was also invited to measure the delay of the portable system antenna cable, as a further check on the consistency of measurements. The results are shown in Table 2.

4. Data processing

Values for the offset between the host and travelling receivers were obtained for each laboratory, as follows.

1. Accurate antenna coordinates are first obtained for the portable system antenna, by submitting RINEX-format self-survey data to the AusPOS online processing service of Geoscience Australia [4]. Table 3 shows coordinates obtained for the portable system antenna at each laboratory in this way. It is hoped that these may be useful as a cross-check of host system antenna coordinates. A full report for each calculation is included in Appendix 2.
2. CCTF data for the portable system is regenerated using the precise antenna coordinates and the stored raw GPS and timing data. Tracks which were invalid for any reason (for example, where either receiver failed to maintain tracking for the full 13 minutes) are discarded.
3. We form the data set

$$\varepsilon(t) = [\text{REF-SV}]_A(t) - [\text{REF-SV}]_B(t) \quad (1)$$

for all valid satellite tracks t common to both receivers A and B; quantities appearing in square brackets are taken from the corresponding data in the CCTF-format file. For the comparison at BNM-SYRTE, we form the difference APMP–OP (that is, we choose $A \equiv \text{APMP}$, denoting the portable receiver, and $B \equiv \text{OP}$) to transfer the calibrated internal delay of the OP receiver to the portable receiver (see (6) below). For all other comparisons we choose A as the host receiver and $B \equiv \text{APMP}$, and use the portable receiver delay to establish a comparison value for the host receiver.

4. We calculate a mean offset $\overline{\varepsilon(t)}$ for the comparison by linear regression (see plots in Appendix 3), where we include a linear as well as a constant term in the fit to $\varepsilon(t)$. The linear term accounts for any slow variation in offset between the two receivers. For completeness, we carry out the regression twice: once with all tracks weighted equally, and once weighting each track t by $[\text{DSG}]_A(t)^{-2}$. The [DSG] values give the RMS scatter of one-second measurements of [REF–GPS] over a 13-minute track [2], and the weighted fit reduces the contribution of tracks with large scatter to $\overline{\varepsilon(t)}$.

Values for $\overline{\varepsilon(t)}$ obtained from both weighted and unweighted fits are shown in Appendix 3. The agreement is very good in all cases, implying that the simple regression is not distorted by any outliers or other anomalies in the data set $\varepsilon(t)$. We therefore adopt the values of $\overline{\varepsilon(t)}$ obtained from the unweighted fits as an appropriate estimate of the mean offset in [REF–SV] between the two receivers.

5. We correct for any difference between delay values as reported by the host laboratory and as used internally by a GPS receiver. This correction is necessary to deal with cases where parameters were measured or corrected after the CCTF data were recorded. ‘Reported’ values are those shown in Appendix 1, and ‘internal’ values are those appearing in the header of the CCTF data files. It should be clearly understood that we take the delays reported by the laboratory as the true values. All delays are summarized in Table 4.

The delay correction applied in processing to generate the CCTF data is

$$[\text{REF-SV}] = (\text{REF-SV})_{\text{Raw}} - [\text{INT DLY}] - [\text{CAB DLY}] + [\text{REF DLY}] \quad (2)$$

so that to account for changes in any of these delay parameters we calculate corrected values $[\text{REF-SV}]'$:

$$[\text{REF-SV}]' = [\text{REF-SV}] + \delta \quad (3)$$

$$\begin{aligned} \delta = & - [\text{INT DLY}]_{\text{Reported}} + [\text{INT DLY}]_{\text{Internal}} \\ & - [\text{CAB DLY}]_{\text{Reported}} - \delta_{\text{AMP}} + [\text{CAB DLY}]_{\text{Internal}} \\ & + [\text{REF DLY}]_{\text{Reported}} - [\text{REF DLY}]_{\text{Internal}} \end{aligned}$$

where δ_{AMP} is an additional correction applied for the line amplifier, if used (§5.5). We follow the convention that [CAB DLY] refers to the delay of the antenna cable only; [INT DLY] includes contributions from the internal delay of both the receiver and antenna, the latter being difficult to measure directly.

Combining (2) and (3) we obtain

$$\begin{aligned} \varepsilon(t)' &= [\text{REF-SV}]_A(t)' - [\text{REF-SV}]_B(t)' \quad (4) \\ &= ([\text{REF-SV}]_A(t) + \delta_A) - ([\text{REF-SV}]_B(t) + \delta_B) \\ &= \varepsilon(t) + \delta_A - \delta_B \end{aligned}$$

so that the mean offset after correcting for delays is

$$\begin{aligned} \overline{\varepsilon(t)'} &= \overline{\varepsilon(t)} + \delta_A - \delta_B \\ &\equiv \Delta \end{aligned}$$

6. If all delays are known we expect the corrected offset Δ to be zero. Any non-zero value can therefore be used to transfer a calibrated value for the internal delay of one receiver to the other. From (3) and (4) we write

$$\begin{aligned} \varepsilon(t)'' &= \varepsilon(t)' - \Delta \text{ so that } \overline{\varepsilon(t)''} = 0 \\ [\text{REF-SV}]_A'' &= [\text{REF-SV}]_A(t)' - [\text{INT DLY}]_{A, \text{True}} + [\text{INT DLY}]_{A, \text{Reported}} \\ [\text{INT DLY}]_{A, \text{True}} &= [\text{INT DLY}]_{A, \text{Reported}} + \Delta \end{aligned}$$

5. Details of data processing for individual laboratories

5.1. NMI (1)

Between 52977 and 53012, the portable system was operated with the line amplifier between the antenna and antenna cable, to estimate the amplifier delay (§5.5). Data in this period were corrected for the measured amplifier delay of $\delta_{\text{AMP}}=0.7$ ns obtained from this data set.

5.2. BNM-SYRTE

The comparison is made in the opposite sense to the other laboratories: the portable receiver internal delay is obtained from the host receiver, rather than the other way around (§4).

5.3. NMI (2)

Between 53093 and 53096, the portable system was operated with the line amplifier between the antenna and antenna cable, to assist with estimating the amplifier delay (§5.5). Data in this period were corrected by the measured amplifier delay of $\delta_{\text{AMP}}=-1.9$ ns obtained from this data set.

5.4. TL

An unknown signal near the GPS L2 frequency was observed at TL during the comparison (Figure 1). Data recorded by both the host and portable receivers show the effects of interference (see Appendix 3). It was possible to identify regions which appeared free of

interference by comparing values for [DSG] and [ISG] to those obtained for similar receivers in other locations. [DSG] and [ISG] give the RMS scatter of one-second values of [REF–GPS] and the measured ionospheric delay [MSIO] (respectively) over a 13-minute track [2]. Data selected in this way are shown in black in the data plots in Appendix 3, and data excluded for suspected interference are shown in a different colour.

5.5. SPRING

For the current comparison, the line amplifier was only used at SPRING, where a long antenna cable was needed for the portable system; all other laboratories used the antenna cable supplied. It is necessary to compensate for any change in apparent antenna cable delay with the line amplifier installed. This change was estimated by measuring the shift in a zero-baseline comparison between the portable and host receivers when the amplifier was inserted and then removed (see Figure 2).

These measurements were made three times at NMI, obtaining delays δ_{AMP} of -0.7 , -1.9 and -0.2 ns. The same cable configuration was used in each case, so that the apparent variation is due to the amplifier only. Note that, based on the data shown in Figure 2, the line amplifier appears to *reduce* the apparent cable delay ($\delta_{AMP} < 0$). A value of $\delta_{AMP} = (-1 \pm 1)$ ns has been adopted for the delay correction to be applied at SPRING.

We note here that we are unable to distinguish between two contributions to δ_{AMP} which both arise in principle: one due to a simple internal delay of the amplifier itself, and the other due to any variation in the internal delay of the receiver as a function of the input GPS signal level. To our knowledge the latter effect has not been measured for any receiver. It is possible that such an effect may account for the sign and moderate scatter of values for δ_{AMP} obtained at NMI. We also note that we are not able to evaluate any possible contribution from this effect due to different GPS reception conditions between NMI, where the delay was measured, and SPRING, where the amplifier was used.

6. Results and discussion

Results are shown in Tables 3–6. We reiterate that these should be regarded as provisional until participating laboratories have had opportunity to review and comment. In particular, any inadvertent error in the delay values shown in Table 4 (for example, any transcription error made during analysis at NMI) will affect the final value obtained for the host receiver internal delay.

6.1. General observations

It is not possible to give an uncertainty in the values obtained for internal receiver delays. This uncertainty includes at least three contributions: uncertainty in the internal delay adopted for the portable receiver obtained from the comparison at BNM-SYRTE, in delay parameters as measured by the host institutes, and in the mean offset obtained from the comparison at each institute. The last contribution should be carefully evaluated with reference to the statistical properties of the corresponding recorded data.

The level of consistency between results obtained for the three comparisons at NMI is very good, with closure to approximately one nanosecond between the beginning and end of the round. This is an encouraging result, and gives confidence in the performance and stability of the portable system. We note that for a recent intercomparison coordinated by BIPM [5], closure was obtained at the level of 4 ns.

6.2. Specific results

The host receiver at NMI, a Topcon Euro-80 dual-frequency receiver, has a nominal internal delay of 46.5 ns. This value is regarded as provisional, as it was obtained by transfer from an AoA TTR6 receiver (serial number 446), and the uncertainty in the internal delay of this receiver is relatively large [7]. The offset obtained for the NMI host receiver consequently appears reasonable.

The agreement with the results of independent comparisons undertaken by BIPM [5, 6] is also encouraging. The most recent comparison obtained a differential correction of $(+9 \pm 4)$ ns to be applied to UTC(AUS) – UTC(OP) [5], or equivalently to the internal delay of the NMI receiver taking the OP receiver as reference. In addition, an earlier comparison obtained a differential correction of $(+8.8 \pm 3.0)$ ns for UTC(KRISS) – UTC(OP) [6]. The nominal value for the KRISS host receiver, an NMI/Topcon dual-frequency receiver, was obtained by transfer from the NMI receiver during commissioning at NMI. All three offsets (this comparison, [5] and [6]) are in good agreement.

We note that this offset obtained for the NMI receiver will also appear as a contribution to the offset obtained for the host receivers at both NICT and SPRING. This is because the reported values for the internal delays of both receivers were similarly obtained by transfer from the NMI receiver during commissioning at NMI. Regarding the remaining offset of approximately 4 ns at SPRING, we observe that the host receiver is a single-frequency Motorola Oncore, and the comparison data consequently exhibits a larger RMS scatter (6 ns, compared to 2 ns typically obtained from dual-frequency receivers in this comparison).

The most likely cause for the relatively large offset obtained for the host receivers at NICT and NMIJ is a misinterpretation by NMI of the delay information provided by these laboratories.

The internal delay of the TL host receiver was also obtained during commissioning at NMI, but in this case by transfer from the BIPM H travelling receiver which was fortuitously hosted by NMI at this time [5]. The offset of 9 ns obtained for the NMI host receiver is therefore not expected. The consistency between values obtained by the two independent comparisons is again good, particularly in view of the closure uncertainty of the BIPM campaign noted above.

6.3. Future intercomparisons

The performance of the new portable receiver appears encouraging. Previous APMP intercomparisons have suffered from poor reliability of the travelling receiver [7]; no such difficulty has been encountered with the portable system in the current round.

Approximately one week of data collection at each host laboratory appears sufficient. No significant changes therefore appear necessary to either the portable system itself or to the comparison procedure for future campaigns.

7. Conclusion

There now exist multiple independent comparisons among receivers at APMP member laboratories (Figure 3). These include comparisons conducted by the APMP itself [7, and this work], by BIPM [5, 6], and by individual laboratories (for example, transfer calibrations undertaken during commissioning of new receivers at NMI). This network provides a wealth of information to assess the consistency of results and to study the stability of receiver delays over time.

We hope that the current intercomparison contributes to maintaining the integrity of time transfer in and beyond the Asia-Pacific region, and we look forward to continuing this important work together in the future.

8. Acknowledgements

The authors wish to express their gratitude to their colleagues in all participating laboratories for their dedicated and highly professional cooperation during the intercomparison. We thank Dr Liao of TL for generously making the portable receiver system available, and we are grateful to Dr Liao and to Dr Imae of NMIJ for their support through the work of the APMP TCTF.

9. References

- [1] P. T. H. Fisk *et al*, 'GPS activities at the National Measurement Institute, Australia', *Proceedings of the Asia-Pacific Time and Frequency Workshop 2004*, Beijing.
- [2] D. W. Allan and C. Thomas, 'Technical Directives for Standardization of GPS Time Receiver Software', *Metrologia* **31** 69–79 (1994).
- [3] <http://www.navcen.uscg.gov/pubs/gps/rinex/>
- [4] <http://www.ga.gov.au/nmd/geodesy/sgc/wwwgps/>
- [5] W. Lewandowski and P. Moussay, *Rapport BIPM-2003/05*.
- [6] W. Lewandowski and L. Tisserand, *Rapport BIPM-2004/06*.
- [7] P. T. H. Fisk and R. B. Warrington, 'Report on the APMP Round Robin GPS Common-View Time Transfer Receiver Intercomparison Experiment': 'Round 1: October 1999 to May 2000', 'Round 2: March 2001 to July 2001', and 'Interim Appendix' (2002).

	Host receiver	Serial number	Start		Stop	
NMI (1)	NMI/Topcon	8RQRFKXT534	52970	27/11/03	53029	25/01/04
BNM-SYRTE	AoA TTR5	051	53062	27/02/04	53075	11/03/04
NMI (2)	NMI/Topcon	8RQRFKXT534	53082	18/03/04	53101	6/04/04
TL	NMI/Topcon	8RJJBWROCG	53115	20/04/04	53128	3/05/04
	AoA TTR6	479				
NICT	NMI/Topcon	8PN45EETDKW	53142	17/05/04	53149	24/05/04
	AoA TTR6	451				
NMIJ	AoA TTR6	484	53151	26/05/04	53156	31/05/04
SPRING	NMI/Oncore		53164	8/06/04	53172	16/06/04
NMI (3)	NMI/Topcon	8RQRFKXT534	53180	24/06/04	53208	22/07/04

Table 1: Schedule of the first round of the intercomparison.

	NML IF delay (ns)	Measurement method
NMI (1)	159.8 ± 1.0	Time-interval counter
BNM-SYRTE		
TL	159.0 ± 1.5	Network analyser
NICT		
NMIJ		
SPRING	158.5 ± 2.0	Time-interval counter
NMI (3)	159.3 ± 1.0	Time-interval counter

Table 2: Values obtained for the delay of the portable system antenna cable from measurements made by host laboratories.

	ITRF2000 @	Cartesian			Geodetic, GRS80 ellipsoid						Baseline (m)
		X (m)	Y (m)	Z (m)	Latitude			Longitude		Height (m)	
NMI (1)	18/12/03	-4648204.271 <i>0.007</i>	2560477.026 <i>0.007</i>	-3526504.952 <i>0.006</i>	-33° -46'	-58.1539" <i>0.001 m</i>	151° 9'	6.1177" <i>0.006 m</i>	99.072 <i>0.010</i>	8.067 <i>0.012</i>	
BNM-SYRTE	1/03/04	420783.525 <i>0.002</i>	171637.812 <i>0.004</i>	4778657.541 <i>0.004</i>	48° 50'	9.1056" <i>0.002 m</i>	2° 20'	5.7574" <i>0.005 m</i>	124.628 <i>0.004</i>	4.687 <i>0.006</i>	
NMI (2)	21/03/04	-4648204.276 <i>0.009</i>	2560477.037 <i>0.008</i>	-3526504.944 <i>0.008</i>	-33° -46'	-58.1534" <i>0.003 m</i>	151° 9'	6.1174" <i>0.004 m</i>	99.076 <i>0.014</i>	8.060 <i>0.014</i>	
TL	24/04/04	-2994425.895 <i>0.010</i>	4951311.783 <i>0.017</i>	2674496.617 <i>0.018</i>	24° 57'	12.8151" <i>0.009 m</i>	121° 9'	52.0875" <i>0.025 m</i>	202.329 <i>0.025</i>	13.592 <i>0.027</i>	
NICT	22/05/04	-3942161.308 <i>0.001</i>	3368285.880 <i>0.001</i>	3701886.725 <i>0.002</i>	35° 42'	23.9392" <i>0.001 m</i>	139° 29'	18.7997" <i>0.000 m</i>	131.323 <i>0.002</i>	4.886 <i>0.002</i>	
NMIJ	28/05/04	-3962302.243 <i>0.002</i>	3308875.364 <i>0.001</i>	3733523.235 <i>0.003</i>	36° 3'	32.0393" <i>0.003 m</i>	140° 8'	6.4005" <i>0.001 m</i>	78.502 <i>0.001</i>	12.763 <i>0.004</i>	
SPRING	11/06/04	-1519458.890 <i>0.013</i>	6192913.814 <i>0.009</i>	142851.472 <i>0.004</i>	1° 17'	31.1958" <i>0.004 m</i>	103° 47'	7.6451" <i>0.013 m</i>	66.579 <i>0.009</i>	7.632 <i>0.016</i>	
NMI (3) †	27/06/04	-4648199.675 <i>0.008</i>	2560483.895 <i>0.017</i>	-3526506.097 <i>0.008</i>	-33° -46'	-58.1976" <i>0.001 m</i>	151° 9'	5.7977" <i>0.014 m</i>	99.117 <i>0.014</i>	0.977 <i>0.020</i>	

† The antenna was placed on a different mount point to that used for NMI (1) and (2).

Table 3: Precise antenna coordinates obtained from self-survey of the portable receiver for each comparison, in the ITRF2000 coordinate frame at the reference time indicated. These coordinates are obtained from RINEX-format data files generated by the portable time-transfer system and submitted to AusPOS, the online service provided by Geoscience Australia. Coordinate uncertainties in metres are shown in italics, and are typically below one centimetre. The baseline shown is the distance between portable and host antennas, where the latter are taken from the header of the CCTF-format data files.

	Host receiver						Travelling receiver						
	Reported			Internal			Reported				Internal		
	INT	REF	CAB	INT	REF	CAB	INT	REF	CAB	AMP	INT	REF	CAB
NMIA (1)	46.5	76.	75.9	46.5	68.9	75.9	33.1	85.9	159.8	0.0	44.79	85.64	159.8
BNM-SYRTE	54.	304.	168.	54.	304.	168.	44.79	306.	159.8	0.0	44.79	85.64	159.8
NMIA (2)	46.5	76.	75.9	46.5	68.9	75.9	33.1	85.9	159.8	0.0	44.79	85.64	159.8
TL	45.1	30.7	119.1	45.1	30.7	119.1	33.1	37.6	159.8	0.0	44.9	37.6	159.8
NICT	47.2	344.123	152.15	47.2	344.123	152.15	33.1	319.97	159.8	0.0	44.9	319.97	159.8
NMIJ	50.	27.	259.	50.	27.	259.	33.1	510.6	159.8	0.0	44.9	510.6	159.8
SPRING	-30.	14.8	344.	-30.	16.	344.	33.1	72.	270.	-1.0	44.9	72.	270.
NMIA (3)	46.5	76.	75.9	46.5	68.9	75.9	33.1	85.9	159.8	0.0	44.79	85.64	159.8

Table 4: Values for receiver delay parameters provided by participating laboratories ('reported') and obtained from the header of the CCTF-format data files ('internal'). The column labelled AMP holds values for the line amplifier delay δ_{AMP} (§5.5).

	Offset					Correction (ns)			
	Tracks	Midpoint	Mean (ns)	RMS (ns)	Slope (ps/day)	Host	Portable	Total	Δ
NMIA (1) – APMP	19526	53000.0	0.6	2.0	-3 \pm 1	7.1	-11.95	-4.85	-4.25
APMP – BNM-SYRTE	539	53068.9	-232.1	2.6	40 \pm 30	0.0	220.36	220.36	-11.74
NMIA (2) – APMP	5809	53091.6	0.6	2.0	-30 \pm 5	7.1	-11.95	-4.85	-4.25
TL – APMP	1342	53121.0	-3.8	0.9	36 \pm 13	0.0	-11.8	-11.8	-15.6
NICT – APMP	2252	53145.6	25.4	1.9	-59 \pm 21	0.0	-11.8	-11.8	13.6
NMIJ – APMP	230	53153.6	52.7	2.4	-56 \pm 104	0.0	-11.8	-11.8	40.9
SPRING – APMP	2691	53168.1	15.4	6.1	-23 \pm 52	-1.2	-12.8	-14.	1.4
NMIA (3) – APMP	9058	53194.6	1.9	2.2	-24 \pm 3	7.1	-11.95	-4.85	-2.95

Table 5: Results obtained from comparison data (see §4). Mean offset, RMS and slope values are obtained from a linear regression to the difference of all common tracks, calculated in the sense indicated, with the mean evaluated at the midpoint. The final mean offset Δ includes corrections for host and portable receivers to account for changes to receiver delay parameters.

	Receiver internal delay (ns)		
	Reported	Δ	Comparison
NMIA (1)	46.5	-4.25	42.3
APMP	44.79	-11.74	33.1
NMIA (2)	46.5	-4.25	42.3
TL	45.1	-15.6	29.5
NICT	47.2	13.6	60.8
NMIJ	50.	40.9	90.9
SPRING	-30.	1.4	-28.6
NMIA (3)	46.5	-3.0	43.6

Table 6: Comparison values for the internal delay for receivers participating in the intercomparison, obtained from the reported value plus the offset Δ from Table 5.

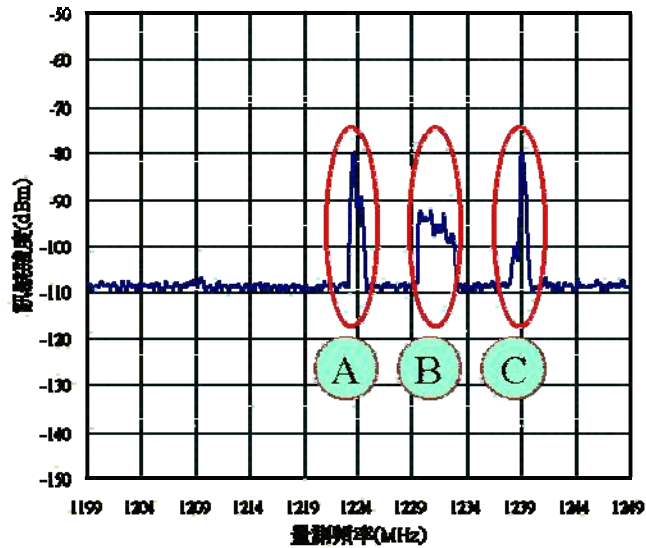


Figure 1: Unknown signal observed at TL near the GPS L2 frequency (1227.6 MHz).

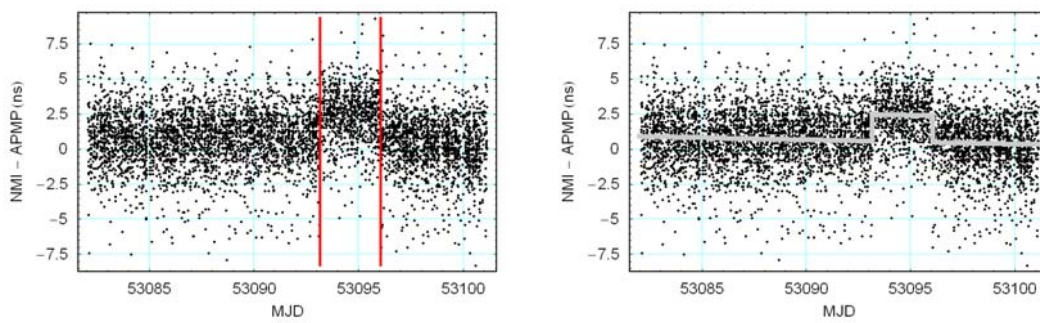


Figure 2: Estimating the delay correction for the line amplifier from a zero-baseline comparison conducted at NMI. The same data are shown in both plots. The solid line at right is a fitted step function with a variable slope. A value of $\delta_{AMP} = -1.9$ ns is obtained from these data.

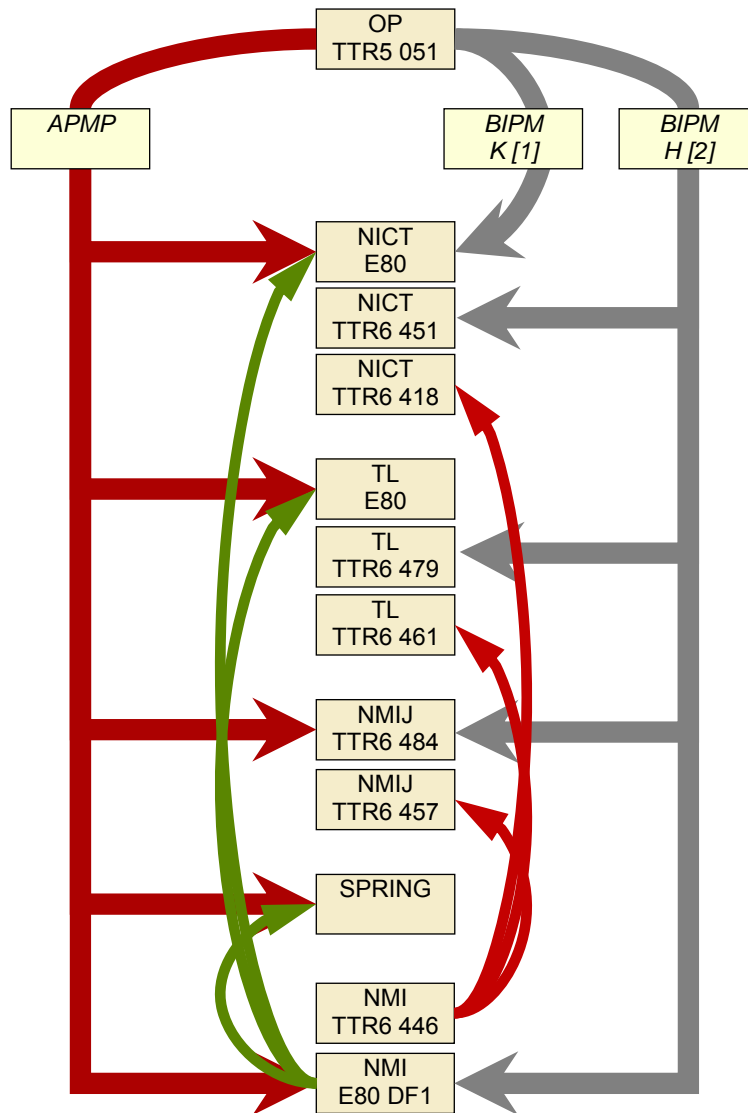


Figure 3: Independent delay comparisons among APMP receivers: — first round of current campaign; — transfer calibration when receiver commissioned at NML; — APMP campaign 1999-2001 (TTR6); — previous BIPM campaigns.